

Field-Induced Mott Transition in a Spin-Gapped Insulator with a Triangular Lattice

Y. Shimizu,^{1,*} H. Akimoto,¹ H. Tsujii,¹ A. Tajima,¹ and R. Kato^{1,2}

¹RIKEN, Wako, Saitama 351-0198, Japan.

²CREST, RIKEN, Wako, Saitama 351-0198, Japan.

(Dated: May 26, 2019)

A bandwidth-controlled Mott transition is investigated by applying hydrostatic pressure to a triangular-lattice Mott insulator, $\text{EtMe}_3\text{P}[\text{Pd}(\text{dmit})_2]_2$, which has a nonmagnetic ground state at ambient pressure. We have observed insulator-to-metal and reentrant metal-to-insulator Mott transitions. Application of a magnetic field dramatically diminishes the reentrant Mott transition in contrast to the Mott insulator with antiferromagnetic order. The result shows that the Mott insulating phase with a finite spin gap exists on the border of superconducting and metallic phases.

PACS numbers: 71.30.+h, 74.25.Nf, 74.70.Kn

The Mott transition has been one of the fundamental issues in solid state physics [1]. Much attention has been paid on the superconducting state near the Mott transition in transition metal compounds [2] and in organic materials [3]. Mott insulators so far studied usually exhibit antiferromagnetic long-range order. When geometrical spin frustration is present, however, novel quantum states such as the resonating valence bond [4] and valence bond solid (VBS) states [5] can be realized. Despite a considerable amount of theoretical work on the quantum antiferromagnets, only a few examples of the VBS state are known in two-dimensional (2D) systems, e.g., $\text{SrCu}_2(\text{BO}_3)_2$ [6] and $\text{BaCuSi}_2\text{O}_6$ [7], and so far the metal-insulator transition has not been accessible experimentally. Hence, the nature of the Mott transition and the superconductivity emerging from the VBS state remains an attractive unsolved problem concerning strongly correlated electrons.

An anion radical salt, $\text{EtMe}_3\text{P}[\text{Pd}(\text{dmit})_2]_2$, is a rare example of a 2D VBS system [8, 9], where Et and Me denote C_2H_5 and CH_3 respectively, and $\text{Pd}(\text{dmit})_2$ ($\text{dmit} = 1,3\text{-dithiole-2-thione-4,5-dithiolate, } \text{C}_3\text{S}_5^{2-}$) is an electron-acceptor molecule. Its crystal structure consists of two layers: the $\text{Pd}(\text{dmit})_2$ layer which involves in conduction and magnetism, and the insulating closed-shell EtMe_3P^+ layer. In the conduction layer, pairs of $\text{Pd}(\text{dmit})_2$ molecules form dimers arranged in a triangular lattice in terms of transfer integrals, t and t' ($t'/t = 1.05$) [see Fig. 1 inset]. The conduction band is half filling, consisting of an anitibonding combination of the highest-occupied molecular orbital of $\text{Pd}(\text{dmit})_2$ [10]. The large onsite Coulomb interaction in the dimer, compared with the bandwidth, produces a Mott-Hubbard insulating state with a spin-1/2 at each dimer site. The $\text{Pd}(\text{dmit})_2$ salt is thus a textbook example of a triangular-lattice quantum antiferromagnet accessible to the Mott transition by bandwidth control. In fact, the magnetic susceptibility of $\text{EtMe}_3\text{P}[\text{Pd}(\text{dmit})_2]_2$ behaves in accordance with the triangular-lattice antiferromagnetic Heisenberg model over a wide temperature range (60 K $< T < 300$ K) with $J = 250$ K [9], indicating the presence

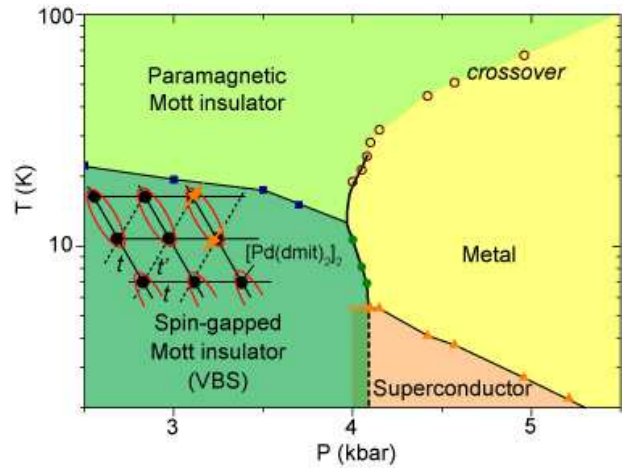


FIG. 1: Pressure-temperature ($P - T$) phase diagram of $\text{EtMe}_3\text{P}[\text{Pd}(\text{dmit})_2]_2$ obtained from resistivity measurements. Open circle: the metal-insulator transition/crossover temperature; solid circle: the insulator-metal transition temperatures (averages between the cooling and warming processes); square: the VBS transitions; triangle: the onset superconducting transition. The dotted line is the expected first-order Mott transition line (see text). Inset shows an illustration of the VBS state in the triangular lattice of $[\text{Pd}(\text{dmit})_2]_2^-$.

of spin frustration and hence highly degenerate ground states. This degeneracy is lifted through a second-order phase transition into a nonmagnetic state at 25 K due to the formation of the VBS with the unit-cell doubling along a molecular stacking direction [8, 9] (see inset of Fig. 1). Application of hydrostatic pressure, which increases the bandwidth, induces a superconducting transition at $T_c = 5$ K [8]. However, understanding of the nature of the insulator and metal phases under pressure and the Mott transition between them remains an intriguing issue.

In this Letter, we report resistivity measurements of $\text{EtMe}_3\text{P}[\text{Pd}(\text{dmit})_2]_2$ at hydrostatic pressures, and construct a pressure-temperature ($P - T$) phase diagram of the Mott transition as shown in Fig. 1. We found that

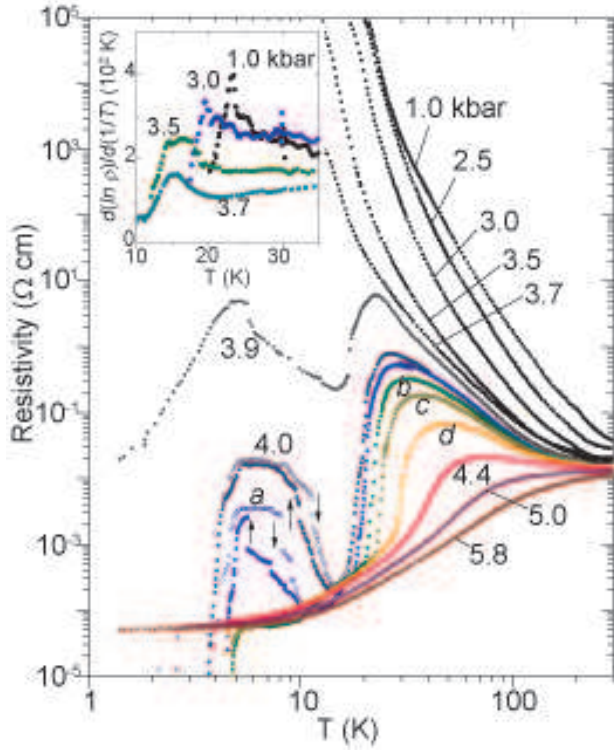


FIG. 2: Temperature dependence of the resistivity of $\text{EtMe}_3\text{P}[\text{Pd}(\text{dmit})_2]_2$ under hydrostatic pressures, where the pressure values are $a = 4.08$, $b = 4.10$, $c = 4.12$, and $d = 4.15$ kbar. The inset shows the activation gap obtained as $\Delta = d(\ln \rho)/d(1/T)$.

the Mott insulating phase borders on a superconducting phase and an unconventional metallic phase that has unusual resistivity behavior, separated by the first-order Mott transition line. The Mott transition is remarkably sensitive to magnetic field, which provides evidence that the spin-gapped Mott insulator persists to the Mott boundary.

Single crystals of $\text{EtMe}_3\text{P}[\text{Pd}(\text{dmit})_2]_2$ were prepared by aerial oxidation of $(\text{EtMe}_3\text{P})_2[\text{Pd}(\text{dmit})_2]$ in acetone containing acetic acid at 5 °C. A hydrostatic pressure was applied to the single crystal at room temperature by using a BeCu pressure-cramp cell with Daphne 7373 as the pressure medium. The denoted pressure values are those applied and calibrated at room temperature by performing simultaneous resistance measurements of the sample and manganin wire. The pressure is known to decrease by 1.5 kbar at low temperatures mainly due to solidification of the pressure medium around 200-250 K but it remains constant below 50 K [11]. The in-plane resistivity was measured using a four-probe method. A magnetic field of up to 16 T was applied nearly parallel to the conducting layer. The temperature or magnetic field was swept below 20 K at rates of 0.1 K/min and 0.032 T/min, respectively.

Figure 2 shows the temperature dependence of the re-

sistivity at various pressures. At pressures below 3.7 kbar, the resistivity is semiconducting over the entire temperature range and does not exhibit thermal hysteresis or a resistance jump. The activation gap given by $\Delta = d(\ln \rho)/d(1/T)$ shows a notable increase and a maximum below 30 K (see inset of Fig. 2). The temperature that exhibits a maximum charge gap (23 K at 1.0 kbar) agrees with the observed VBS transition temperature for the magnetic susceptibility at ambient pressure [9], and decreases to 15 K when the pressure is increased up to 3.7 kbar (indicated by the solid squares in Fig. 1). This result indicates that the spin gap decreases gradually as the Mott-Hubbard gap is reduced by increasing the pressure.

At 4.0 kbar, an abrupt drop in the resistivity of more than three orders of magnitude is observed in a narrow temperature range, $17 \text{ K} < T < 20 \text{ K}$, indicating a first-order insulator-to-metal (IM) Mott transition in the bulk crystal as typically observed for the bandwidth-controlled Mott transition [12, 13, 14]. Once the resistivity settles into metallic behavior, it increases again below 13 K. A resistivity jump and a thermal hysteresis are manifestations of the first-order metal-to-insulator (MI) phase transition. Finally, a superconducting transition is observed at 5.3 K. At an intermediate pressure of 3.9 kbar, we observed a similar resistivity profile below 20 K. The much higher resistance values than those at 4.0 kbar probably arises from the formation of metallic current paths in the predominant insulating phase and reflects the first-order nature of the Mott transition and/or slight pressure inhomogeneity in the sample. Upon increasing the pressure further, the IM transition temperature shifts to higher temperatures and becomes a crossover above 4.15 kbar, while the reentrant transition is rapidly suppressed and disappears at 4.1 kbar. Above 5 kbar, the resistivity becomes metallic in all the measured temperature range.

The $P - T$ phase diagram (Fig. 1) summarizes the resistivity measurements. The IM transition (or crossover) temperatures, indicated by the inflection point having the largest value of $d\rho/dT$, are plotted as open circles in Fig. 1, while the reentrant MI transition temperatures (defined as the temperature exhibiting a largest resistance jump) are plotted as solid circles. The onset superconducting transition temperature decreases with increasing pressure at a rate of - 2.5 K/kbar. The superconducting transition from the reentrant insulating state (denoted by open triangles in Fig. 1) should not occur in the bulk sample but in superconducting domains percolated in the insulating phase as seen in $\kappa(\text{ET})_2\text{Cu}[\text{N}(\text{CN})_2]\text{Cl}$ [13, 14]. This is because the metal-superconductor transition is of second order, and then the first-order transition line separating the insulator and superconductor phases (indicated by the dotted line in Fig. 1) should be continuously connected to the line separating the insulator and metal phases, dropping verti-

cally toward $T = 0$.

It is noteworthy that the slope of the first-order Mott transition line is positive at high temperatures but becomes negative at low temperatures. A similar profile is commonly seen in Mott insulators having long-range antiferromagnetic order, e.g., V_2O_3 [12] and κ -(ET)₂Cu[N(CN)₂]Cl [13, 14], but it is in sharp contrast to that of a paramagnetic Mott insulator, κ -(ET)₂Cu₂(CN)₃ [15], having a positive dT/dP slope for all pressure range [16]. From a thermodynamical viewpoint, the slope of the first-order line is described by a Clausius-Clapeyron relation [17], $dT/dP = \Delta V/\Delta S$, where $\Delta V = V_{\text{ins}} - V_{\text{metal}}$ and $\Delta S = S_{\text{ins}} - S_{\text{metal}}$ are the volume and entropy differences between insulator and metal, respectively. Since the metallic state appears on the high-pressure side ($\Delta V > 0$), a negative dT/dP requires the insulating phase to have smaller entropy than the metallic phase ($\Delta S < 0$). It is reasonable that, although the entropy reduction in reentrant Mott insulators arises from the magnetic order in the majority of cases, in the present case it arises from the short-range spin order with a translational symmetry breaking and a spin gap. Application of a magnetic field would affect the magnetism of the Mott insulating state, and eventually the Mott transition.

We have measured the magnetic-field dependence of resistivity in the reentrant insulating phase at a pressure of 4.08 kbar. Figure 3 shows the temperature dependence of the resistivity for several magnetic fields up to 16 T on (a) cooling and (b) warming up. In the absence of a magnetic field, the reentrant MI transition occurs principally at 5.6 K upon cooling, while the insulating state persists up to 8 K in the warming process. When a magnetic field is applied, the MI transition shifts considerably to lower temperatures. Above 10 T, the MI transition disappears for both the cooling and warming processes. The results of the magnetic-field and temperature dependence of resistivity are summarized in the $H - T$ phase diagram shown in the inset of Fig. 3(a), which implies that an isothermal field sweep can induce the Mott transition. Figure 4 shows the magnetoresistivity at $T = 4.2$ K and $P = 4.08$ kbar. Starting from a zero-field-cooled state, the resistivity increases with magnetic field due to the destruction of superconductivity. Once the system enters the high resistivity state, no indication of the insulator-metal transition is seen up to 16 T, reflecting the metastable nature of the insulating phase. On the other hand, after cooling to 4.2 K in a magnetic field of 16 T, a downward field sweep from 16 T shows a resistivity jump at 7 T, indicating a field-driven MI transition. This effect of the magnetic field on the Mott transition is opposite to what was observed in a Mott insulator having antiferromagnetic order [18] and that predicted for a strongly-interacting ³He system [19], in which the insulating phase appears at a high-field side.

The field-induced MI transition can be understood in

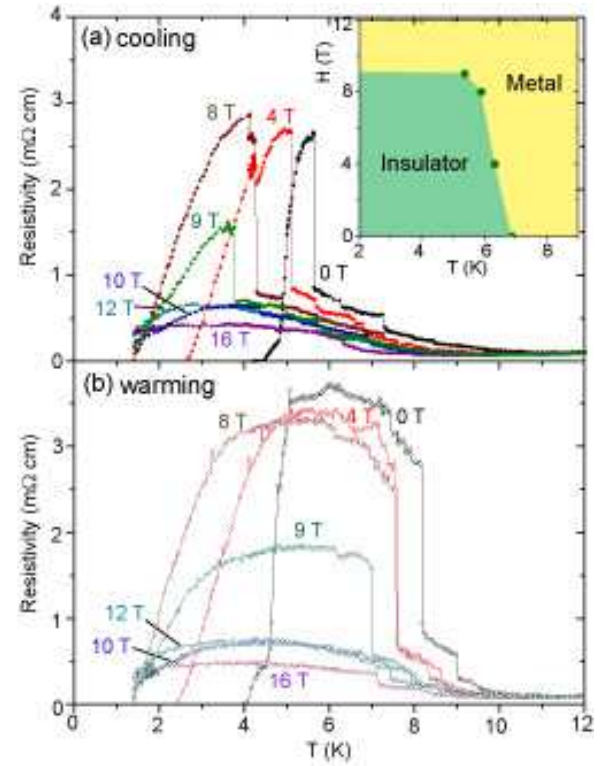


FIG. 3: Magnetic-field dependence of the resistivity at 4.08 kbar for (a) cooling and (b) warming processes. The inset in (a) shows $H - T$ phase diagram, where the averaged MI transition temperatures between the warming and cooling processes are plotted. The percolated superconducting phase below the MI transition temperature is omitted for clarity.

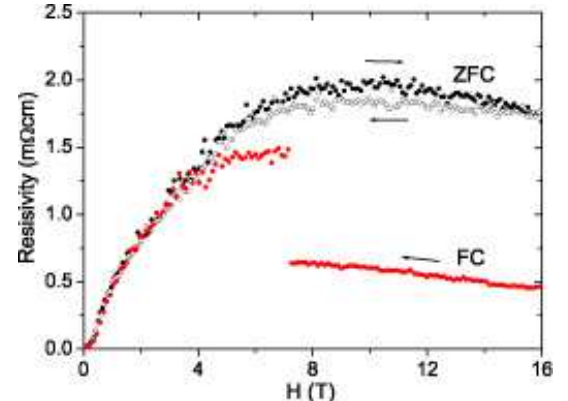


FIG. 4: Magnetoresistivity measured at 4.2 K and 4.08 kbar for zero-field-cooling (ZFC) and field-cooling (FC) at 16 T.

terms of the $H - T$ phase diagram in Fig. 3 (a) as follows. In the analogy of the Clausius-Clapeyron relation, the slope of the phase boundary is expressed as $dH/dT = -\Delta S/\Delta M$, where $\Delta M = M_{\text{ins}} - M_{\text{metal}}$ is the difference in magnetization between the insulating and metallic phases. As has already been shown, $\Delta S = S_{\text{ins}} - S_{\text{metal}} < 0$. The fact that $dH/dT < 0$ in Fig. 3(a) requires $\Delta M < 0$;

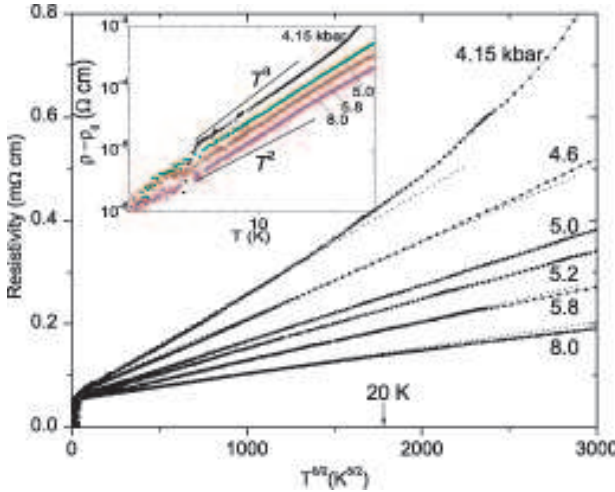


FIG. 5: Resistivity plotted as a function of $T^{5/2}$ in the metallic state. The inset shows $\log(\rho - \rho_0)$ vs $\log T$ plots at selected pressures below 30 K.

that is, the magnetization of the insulating phase must be smaller than that of the metallic phase. This is consistent with the existence of a spin gap in the reentrant insulating state. Namely, the metallic state appears when the Zeeman energy diminishes the spin gap of the reentrant insulating state, instead of the spin-frustrated paramagnetic insulator having a large spin entropy. The critical field, $H_c = 9-10$ T, for the IM transition yields a spin gap given by $\Delta_{\text{VBS}} = g\mu_B H_c = 7-8$ K. Moreover, the clear thermal hysteresis in the MI transition, which is not observed in the IM transition at 20 K, implies the coincidence of the structural transition at the MI transition.

From the shape of the $P - T$ phase diagram and the magnetic field effect on the Mott transition, we conclude that the VBS Mott insulating state is realized on the border of the superconducting state, which has not been observed in Mott insulators previously studied. The metal/superconducting state appearing from the VBS Mott insulator may have an intriguing nature. In order to gain further insight into the metallic state, we discuss the metallic resistivity behavior at low temperatures, which reflects low-energy electron excitations. The $\log(\rho - \rho_0)$ vs $\log T$ plots (where ρ_0 is the residual resistivity) in the inset of Fig. 5 show that the resistivity follows a power law, $\rho = \rho_0 + T^\epsilon$, for a wide range of pressures (4.15-8.0 kbar) at temperatures below 20-30 K and above T_c . The exponent ϵ is in the range, $2 < \epsilon < 3$. Good linearity is found when the resistivity is plotted against $T^{5/2}$ as the main panel of Fig. 5 shows. In a metal with strong electron correlation, the low-temperature resistivity is dominated by electron-electron scattering resulting in $\epsilon = 2$ term for the resistivity in a standard Fermi liquid, as is observed for some organic conductors [16, 20]. A deviation from $\epsilon = 2$ to a larger value is unusual with only a few

known examples [21], while a deviation to a lower value ($1 < \epsilon < 2$) is known in heavy fermion systems located near the quantum critical point [22] and cuprate superconductors [2]. The present result suggests the realization of an anomalous Fermi liquid with emergent low-energy properties or a non-Fermi liquid including spin-charge separation. A possible cause of the anomalous ϵ value is fluctuations in the lattice dimerization and the short-range spin ordering toward the VBS insulating and/or superconducting states. However, it should be noted that the $\epsilon = 5/2$ behavior is observed even at 8.0 kbar, which is far from the Mott transition. This suggests that the ϵ value is unlikely to be due to critical fluctuations.

In conclusion, we have discovered a new type of the pressure-temperature phase diagram for a Mott transition in the triangular-lattice system, $\text{EtMe}_3\text{P}[\text{Pd}(\text{dmit})_2]_2$. In contrast to the other Mott insulators having magnetic order, application of a magnetic field suppresses the insulating state, which provides evidence of a finite spin gap in the insulating state even on the verge of the Mott transition. The metallic state occurring from the VBS state was found to have a novel nature with an unconventional power-law temperature dependence in resistivity.

We thank discussions with M.Imada, S.Watanabe, T.Itou, M.Tamura, N.Tajima, Y.Ishii. This work was supported by Grant-in-Aid for Scientific Research(No.16GS0219) from MEXT and JSPS.

* Electronic address: yasuhiro@riken.jp

- [1] N. F. Mott, *Metal-Insulator Transition*, Tayer and Francis, London (1990).
- [2] M. Imada, *et al.*, Rev. Mod. Phys. **70**, 1039 (1998).
- [3] K. Kanoda, J. Phys. Soc. Jpn. **75**, 051007 (2006).
- [4] P. W. Anderson, Mater. Res. Bull. **8**, 153 (1973); R. Moessner *et al.*, Phys. Rev. Lett. **86**, 1881 (2001); H. Morita, *et al.*, J. Phys. Soc. Jpn. **71**, 2109 (2002).
- [5] N. Read, *et al.*, Phys. Rev. Lett. **62**, 1694 (1989); F. Becca, *et al.*, *ibid.* **89**, 37204 (2002). Z. Weihong, *et al.*, Phys. Rev. B **59**, 14367 (1999);
- [6] H. Kageyama, *et al.*, Phys. Rev. Lett. **82**, 3168 (1999).
- [7] S. E. Sebastian, *et al.*, Nature **441**, 617 (2006).
- [8] R. Kato, *et al.*, J. Am. Chem. Soc. **128**, 10016 (2006).
- [9] M. Tamura, *et al.*, J. Phys. Soc. Jpn. **75**, 093701 (2006).
- [10] R. Kato, Chem. Rev. **104**, 5319 (2004).
- [11] K. Murata, *et al.*, Rev. Sci. Instrum. **68**, 2490 (1997).
- [12] D. B. McWhan, *et al.*, Phys. Rev. B **7**, 1920 (1970); P. Limelette, *et al.*, Science **302**, 89 (2003).
- [13] S. Lefebvre, *et al.*, Phys. Rev. Lett. **85**, 5420 (2000).
- [14] F. Kagawa, *et al.*, Phys. Rev. B **69**, 64511 (2004).
- [15] Y. Shimizu, *et al.*, Phys. Rev. Lett. **91**, 107001 (2003).
- [16] K. Kurosaki, *et al.*, Phys. Rev. Lett. **95**, 177001 (2005).
- [17] S. Watanabe, *et al.*, J. Phys. Soc. Jpn. **73**, 3341 (2004).
- [18] F. Kagawa, *et al.*, Phys. Rev. Lett. **93**, 127001 (2004).
- [19] D. Vollhardt, Rev. Mod. Phys. **56**, 99 (1984); L. Laloux, *et al.*, Phys. Rev. B **50**, 3092 (1994).

- [20] P. Limelette, *et al.*, Phys. Rev. Lett. **91**, 0160401 (2003).
- [21] T. Itou, *et al.*, Phys. Rev. Lett. **93**, 216408 (2004).
- [22] G. R. Stewart, Rev. Mod. Phys. **73**, 797 (2001).